Effect of UV-Photocrosslinking on the Nonisothermal Crystallization Kinetics of Polyethylene

Longxiang Tang,[1] Manqing Yan,[2] Chunhua Liu,[1] Pinghua Wang,[1] Baojun Qu[3]

[1]*Department of Polymer Science and Engineering, Hefei University of Technology, Hefei, Anhui 230009, People's Republic of China*
[2]*School of Chemistry, Anhui University, Hefei, Anhui 230039, People's Republic of China*
[3]*Department of Polymer Science and Engineering, University of Science and Technology of China, Hefei, Anhui 230026, People's Republic of China*

Received 6 September 2006; accepted 27 July 2007
DOI 10.1002/app.27617
Published online 27 December 2007 in Wiley InterScience (www.interscience.wiley.com).

ABSTRACT: The influences of UV-photocrosslinking on crystallite structure and nonisothermal crystallization kinetics of polyethylene (PE) were investigated by optical microscope (OM) and differential scanning calorimetry (DSC) at different cooling rates, respectively. The observation of crystallite structure showed that, due to crosslinking of molecular chains of PE, the PE spherulites grow more imperfectly with increasing gel content. The Avrami analysis modified by Jeziorny was applied to describe the nonisothermal crystallization process of virgin PE and photocrosslinked PE (XLPE) samples. The values of half-time of crystallization $t_{1/2}$ and the parameter Z_c showed that the crystallization rate increased with increasing cooling rates for both XLPE and virgin PE, but the crystallization rate of XLPE is lower than that of virgin PE at the same cooling rate. The activation energies were estimated by the Kissinger method, and the values were 176.7 and 197.1 kJ/mol for virgin PE and XLPE, respectively, indicating that UV-photocrosslinking might hinder the overall nonisothermal crystallization process of PE. © 2007 Wiley Periodicals, Inc. J Appl Polym Sci 108: 174–180, 2008

Key words: polyethylene; UV-photocrosslinking; nonisothermal crystallization kinetics; optical microscope; differential scanning calorimetry

INTRODUCTION

Polyethylene (PE) is the thermoplastic material produced in the largest quantities in the world, but one of its major drawbacks is a relatively low upper use temperature. It is well known that a modest crosslinking of PE can considerably improve its thermal stability, mechanical properties and its resistance to electrical discharge, solvents, creep and environmental stress-cracking.[1] There are two crosslinking methods: radiation crosslinking (such as γ-rays,[2] electron beam,[3] and UV[4]) and chemical reaction (with peroxide[5] or alkoxy silane[6]). However, photoinitiated crosslinking of PE by UV-irradiation has several inherent advantages, for example, UV-photocrosslinking is highly efficient, there is little degradation or oxidation of the polymer during the UV-crosslinking process, UV-light sources are readily available and easy to handle, and the investment cost is low.[4] Qu and Rånby had systemically studied the mechanism and kinetics of photocrosslinking of PE,[4,7–10] crystallization behaviors, and the application of photocrosslinked PE.[1,11,12] In the recent years, photoinitiated crosslinking technology by UV-irradiation has been used extensively for electrical insulation of wire and cables, hot water piping, heat-shrinkable tubing, film, and foam.[1] It is well known that physical and mechanical properties of crystalline polymers depend on the morphology, the crystalline structure, and the degree of crystallinity. The behavior of thermoplastic semicrystallinity polymers during nonisothermal crystallization from the melt is of increasing technology importance.[13] As far as we know, however, few publications have been dedicated to the studies of nonisothermal crystallization kinetics of photocrosslinked PE thus far.[14,15]

The purpose of this article is to investigate the effects of photocrosslinking of PE on its crystallite structure and nonisothermal crystallization kinetics by means of OM and DSC. The Avrami analysis modified by Jeziorny was applied to describe the nonisothermal crystallization process of PE and XLPE samples. Moreover, the activation energies of virgin PE and XLPE describing the overall crystallization process under nonisothermal condition were also calculated based on Kissinger method.

EXPERIMENTAL

Materials

High-density polyethylene (HDPE, 5000S, melt flow rate = 2.6 g/10 min) was supplied by Yangzi Petro-

Correspondence to: L. Tang (tlx760828@ustc.edu).

Journal of Applied Polymer Science, Vol. 108, 174–180 (2008)

chemical (China). Benzil dimethyl ketal (BDK), supplied by Jingjiang Chemical Engineering (China), was used as a photoinitiator. Triallyl isocyanurate (TAIC) was supplied by Anhui Institute of Chemical Engineering (China) as a crosslinking agent. All materials were used as received without further purification.

Preparation of samples

HDPE was mixed with 1 wt % BDK and 2 wt % TAIC for 8 min at 64 rpm at 150°C by using a Brabender-like apparatus. Then the mixture was hot pressed to sheets of 1-mm thickness at 170°C and 10 MPa pressure for 10 min by using a press. The resulting sheets were irradiated in a UV-cure device constructed in our laboratory.[4] The irradiation source was a medium pressure mercury lamp (Philips HPM 15), operated at 2 kW, at a distance of 10 cm from the surface of the sheets. The irradiation power measured on the surface of the sheets, by means of a radiometer, was of 4.0×10^{-2} W/cm^{-2}. The exposure was carried out in air at a temperature of about 150°C. The sheets were irradiated for different times, and the photocrosslinked PE was designated as PE*n*, where the number *n* denotes UV-irradiation time, for example, PE0 represents virgin PE, while PE20 indicates PE was UV irradiated for 20 s.

Analysis of samples

Determination of gel content

The gel content was measured for the samples after irradiation according to the literature.[4]

Observation of the spherulitic structure

An optical microscope (OM; Model Nikon YS-2, Nikon, Japan) attached to a Nikon camera (Nikon coocpix995) was used to observe the spherulitic structure of virgin PE and XLPE. The films were sandwiched between a microscope slide and a cover glass, after melting at 230°C for 2 min, and then kept in a thermostat at 110°C for 24 h to crystallize isothermally.

Nonisothermal DSC analysis

A PerkinElmer DSC-2C instrument was used for measuring nonisothermal crystallization kinetics in the cooling mode from the molten state (melt crystallization). All measurements were carried out under nitrogen atmosphere. For nonisothermal melt crystallization, the raw sample was heated up rapidly to 180°C and maintained at this temperature for 5 min to remove thermal history. Then the sample was cooled at constant rates of 5, 10, 20, and 40°C/min, respectively. The exothermic crystallization peak was recorded as a function of temperature.

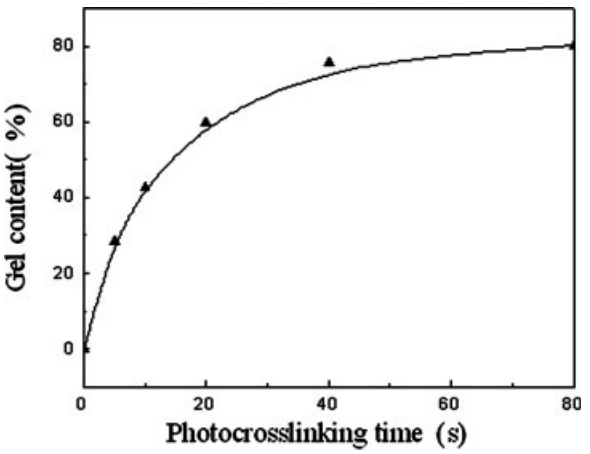

Figure 1 Effect of photocrosslinking time on the gel content of XLPE samples.

RESULTS AND DISCUSSION

Effect of photocrosslinking time on the gel content of XLPE

The effect of photocrosslinking time on the gel content of XLPE is shown in Figure 1. It is evident that the gel content increases rapidly at first and then increases slightly with increasing photocrosslinking time. To elucidate the effect of the extent of photocrosslinking on the nonisothermal crystallization kinetics of PE, we chose PE0 and PE20, which is of medium gel content, about 55%, for nonisothermal crystallization kinetics studies.

Crystallite structure

POM was used to observe the change in crystallite feature resulting from photocrosslinking. Figure 2 shows the polarized optical micrographs of virgin PE and XLPE.

From the virgin PE image, the well-defined spherulites with sharp spherulite boundaries were observed. However, when PE was photocrosslinked, the spherulites appeared increasingly disturbed proportional to photocrosslinking time, indicating that the photocrosslinking of PE impedes its overall crystallization process.

Crystallization behavior of virgin PE and XLPE

The crystallization exothems of virgin PE and XLPE at various cooling rates are presented in Figure 3.

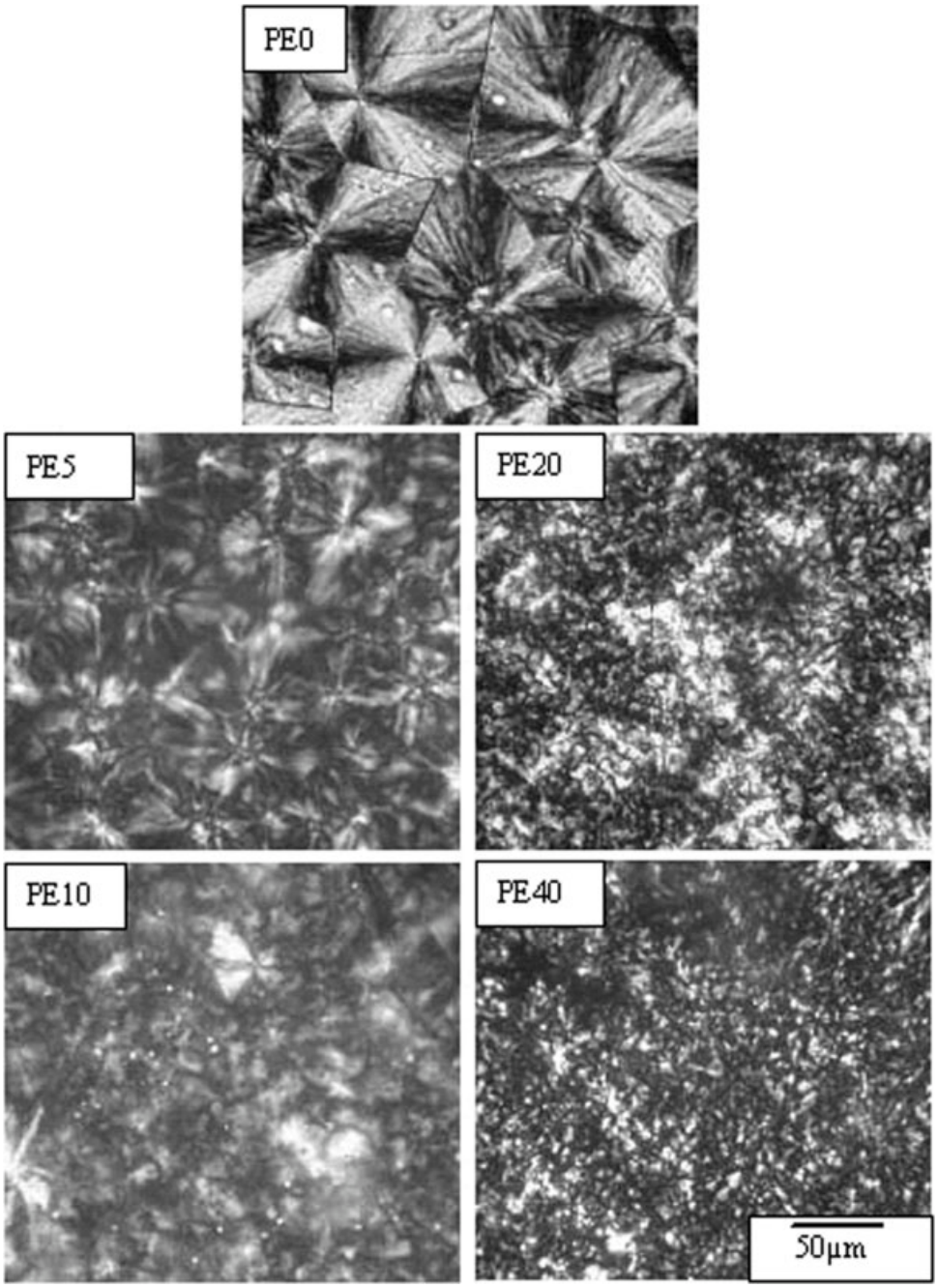

Figure 2 POM images of virgin PE and XLPE samples (×400).

From these curves, some useful parameters, such as the peak temperature (T_p) and the crystallization enthalpy (ΔH_c) of nonisothermal crystallization exotherms, could be obtained, and the results are summarized in Table I. First, T_p shifts, as expected, to a low temperature with increasing cooling rate for both PE0 and PE20, which is attributed to the lower time scale that allows the polymer to crystallize as the cooling rate increases, therefore, a higher undercooling was required to initiate crystallization. On the other hand, the motion of PE molecules could not follow the cooling temperature when the specimens were cooled down fast. Second, for a given cooling rate, T_p of PE20 is lower than that of PE0, indicating that the photocrosslinking hinder crystallization process of PE. A reasonable explanation is that PE, after the crosslinking, forms a net structure, which makes the macromolecule chains less flexible, and consequently the crystallization becomes more difficult, therefore, a higher undercooling was required to initiate crystallization, resulting in lower T_p. As far, ΔH_c, which is proportional to the degree of crystallinity, its values decreased for both PE0 and PE20 as the cooling rate increased. However, in com-

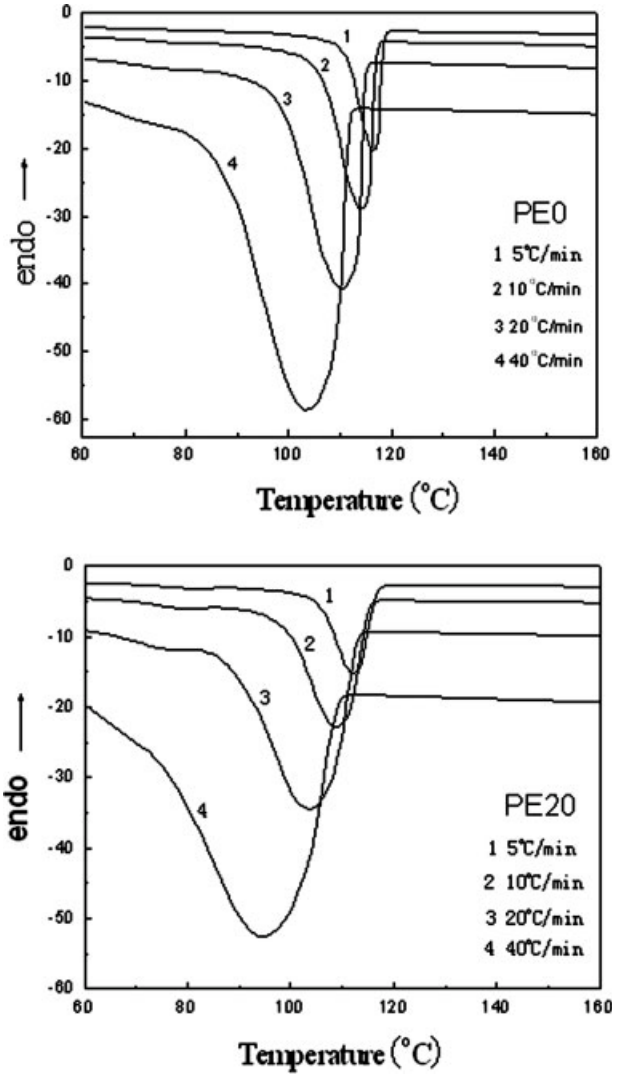

Figure 3 DSC thermograms of nonisothermal crystallization for PE0 and PE20 samples at 5, 10, 20, and 40°C/min, respectively.

parison with PE0, ΔH_c of PE20 is lower. It is reasonable because the crosslinking modifies the molecular structure and hinders the growth of crystal, which is obvious from Figure 3. These results agree well with the reports in the literatures.[16,17]

Nonisothermal crystallization kinetics analysis

Based on Figure 3, integration of the exothermal peaks during the nonisothermal crystallization process can give the relative degree of crystallinity (X_t) as a function of the crystallization temperature T:

$$X_t = \int_{T_0}^{T} (dH_c/dT)dT \Big/ \int_{T_0}^{T_\infty} (dH_c/dT)dT \qquad (1)$$

where T_0 and T_∞ are the onset and end of crystallization temperature, respectively. Figure 4 shows X_t as a function of temperature for PE0 and PE20 at various cooling rates. All of these curves have the same sigmoidal shape, indicating that the lag effect of the cooling rate on crystallization was observed only. Using the following equation: $t = (T_0 - T)/\phi$ [where T is the temperature at crystallization time t, T_0 is the initial temperature as crystallization begins ($t = 0$), and ϕ is the cooling rate]. The value of T on X-axis in Figure 4 can be transformed into crystallization time t as shown in Figure 5. It is obvious from the plots that the higher the cooling rate, the shorter the time needed for the completion of the crystallization process. The half-time of noniosthermal crystallization $t_{1/2}$ could be estimated from Figure 5 for PE0 and PE20, and the results are listed in Table I. As expected, the value of $t_{1/2}$ decreases with increasing cooling rates for both PE0 and PE20. However, the value of $t_{1/2}$ for PE0 is lower than that for PE20 at a given cooling rate, signifying that the photocrosslinking could hinder the overall crystallization process, which is well in accordance with the analyses of crystallite structure by means of OM.

It is well known that the isothermal crystallization kinetics of polymers is commonly studied by the Avrami method.[18]

$$1 - X_t = \exp(-Z_t t^n) \qquad (2)$$

where the exponent n is a mechanism constant depending on the type of nucleation and growth rate parameters, Z_t is a crystallization rate constant,

TABLE I
Nonisothermal Crystallization Kinetic Parameters of Virgin PE and XLPE Samples

Samples	ϕ (K/min)	T_{conset}[a] (°C)	T_p (°C)	n	Z_c	$t_{1/2}$ (min)	ΔH_c (J/g)
PE0	5	119.5	116.4	15.7	0.03	315	71.6
	10	118.0	114.5	8.71	0.05	114	66.3
	20	116.0	110.6	5.46	0.75	60	62.1
	40	112.9	103.8	3.35	5.58	32	58.7
PE20	5	118.0	112.1	12.68	0.02	366	65.4
	10	116.2	109.0	7.71	0.03	144	59.3
	20	114.5	103.8	5.53	0.55	78	52.6
	40	111.0	94.4	3.59	1.90	46	49.8

[a] T_{conset}, the onset temperature of crystallization.

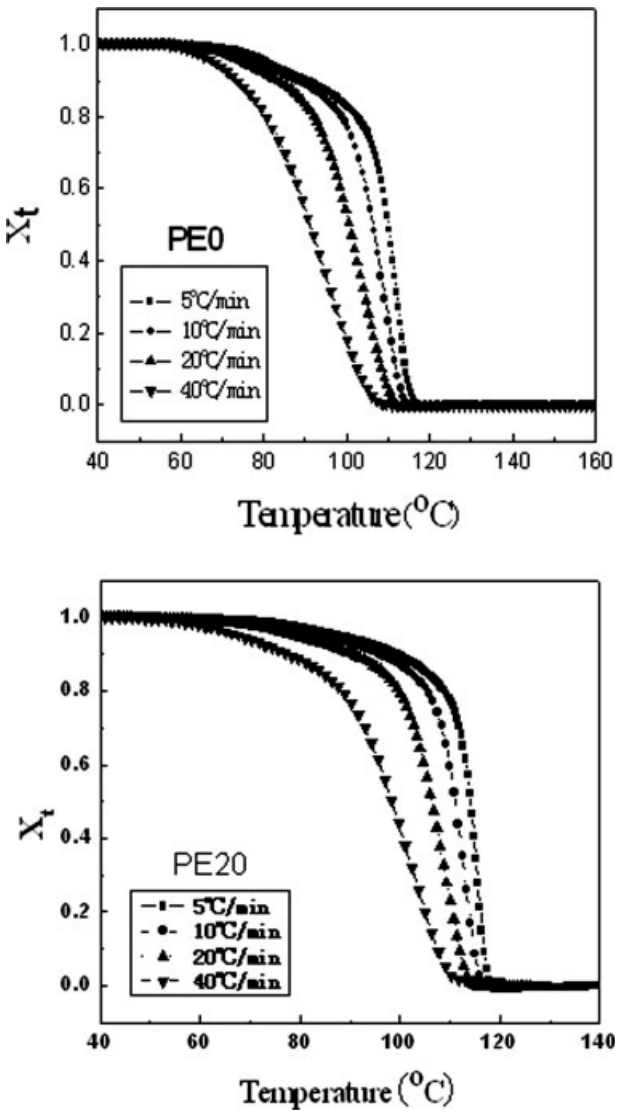

Figure 4 Plots of X_t versus T for PE0 and PE20 samples during nonisothermal crystallization process.

and t is the time taken during the crystallization process. Using eq. (2) in double-logarithmic form:

$$\ln(-\ln(1 - X_t)) = \ln Z_t + n \ln t \tag{3}$$

and plotting $\ln(-\ln(1 - X_t))$ versus $\ln t$ for each cooling rate, a straight line is obtained (see Fig. 6). From the slope and intercept of the lines, n and Z_t can be determined. However, it should be taken into account that, during nonisothermal crystallization process, Z_t and n do not have the same physical significance as in the isothermal crystallization, due to the fact that during nonisothermal crystallization process the crystallization temperature is lowered continuously. This consequently affects the rates of both nuclei formation and spherulite growth because they are temperature dependent. Jeziorny presented the final form of the parameter characterizing the kinetics of nonisothermal crystallization as follows[19]:

$$\ln Z_c = \ln Z_t / \phi \tag{4}$$

The results obtained from Avrami plots and Jeziorny method are listed in Table I. For both PE0 and PE20, as expected, the value of Z_c increases with increasing cooling rates. However, the value of Z_c at a given cooling rate for PE20 is lower than that of PE0, which further indicates that the photocrosslinking hinders the overall crystallization process of PE. Moreover, this result is consistent with the analysis of $t_{1/2}$. The exponent n is quite scattered, which is

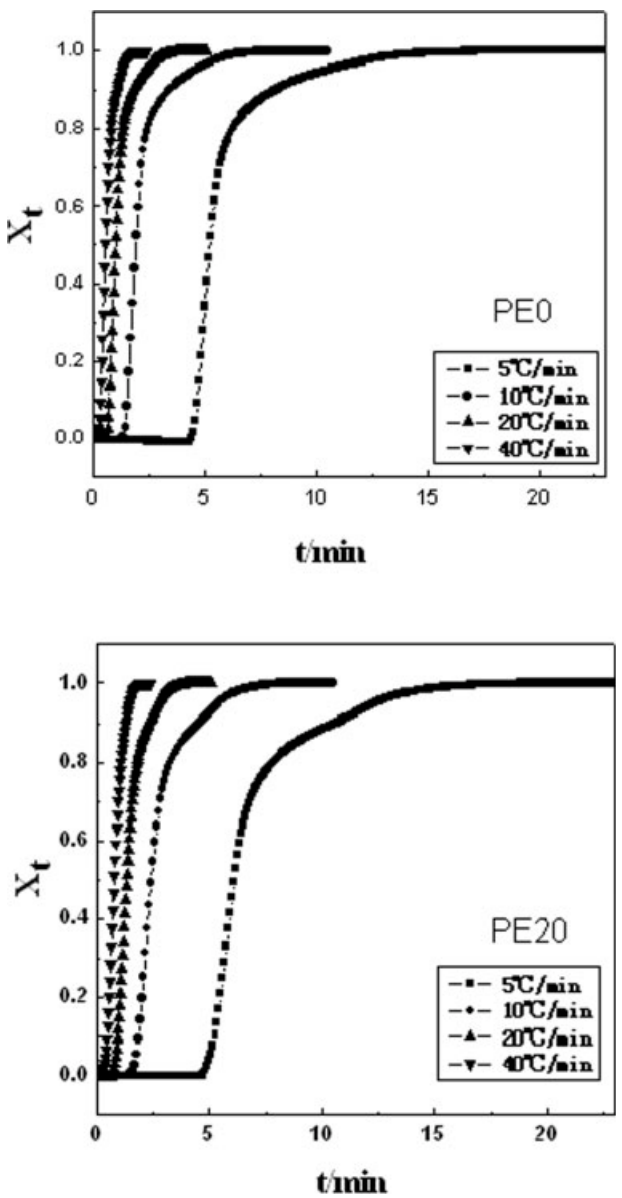

Figure 5 Plots of X_t versus t for PE0 and PE20 samples during nonisothermal crystallization process.

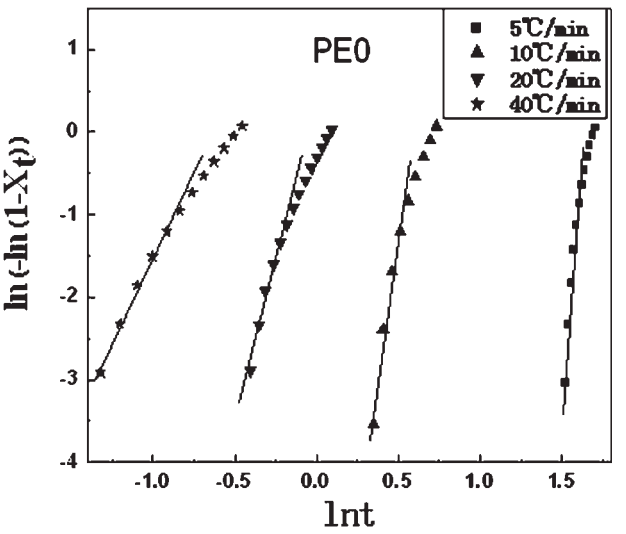

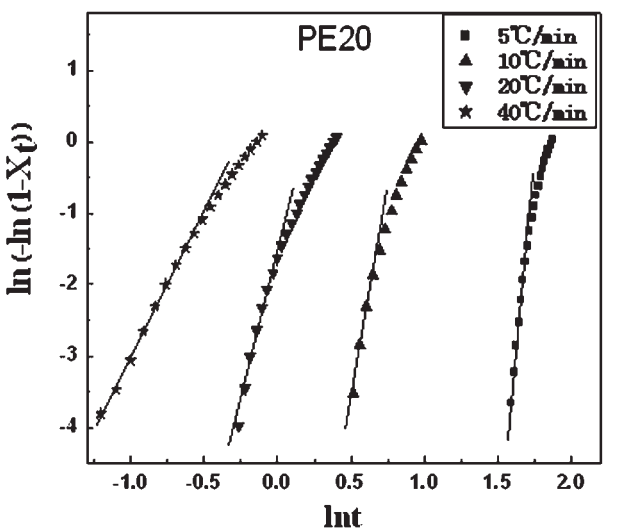

Figure 6 Plots of $\ln(-\ln(1 - X_t))$ versus $\ln t$ for PE0 and PE20 samples during nonisothermal crystallization process.

different from those of the Avrami exponent obtained from the isothermal crystallization analysis. It is reasonable because nonisothermal crystallization is a dynamic process in which the crystallization rate is no longer constant but a function of time and cooling rate. Also, nucleation may be more complicated than that of isothermal crystallization. These factors could make the exponent n fractional and not have a narrow spread.

Effective activation energy describing the overall crystallization process

Considering the variation of the peak temperature T_p with the cooling rate ϕ, the effective activation energy ΔE can be calculated on the basis of eq. (5) was proposed by Kissinger.[20]

$$\frac{d\left[\ln\left(\phi/T_p^2\right)\right]}{d(1/T_p)} = \frac{\Delta E}{R} \tag{5}$$

where R is the universal gas constant, $\ln(\phi/T_p^2)$ versus $1/T_p$ is plotted to obtain a line (see Fig. 7), the slope of the curve determines $\Delta E/R$, thus ΔE can be calculated accordingly. The calculated values of ΔE are listed in Table II. It is clear that, ΔE of PE20 is higher than that of PE0. Accordingly, photocrosslinking may hinder the overall nonisothermal crystallization process of PE, which confirms with the analysis of T_p, $t_{1/2}$, Z_c, and crystallite structure.

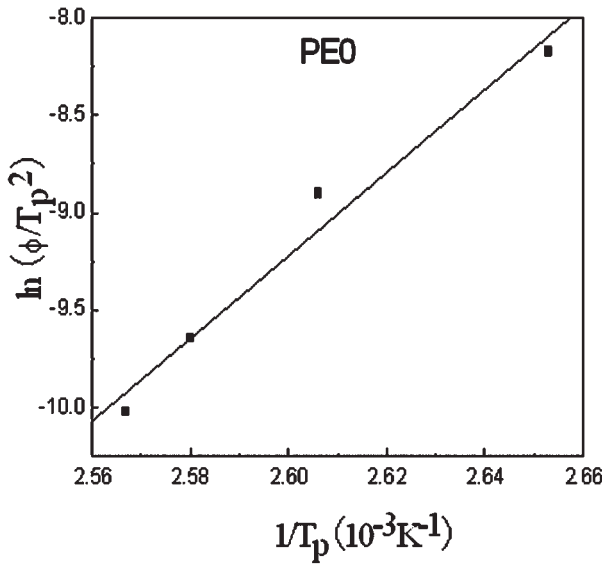

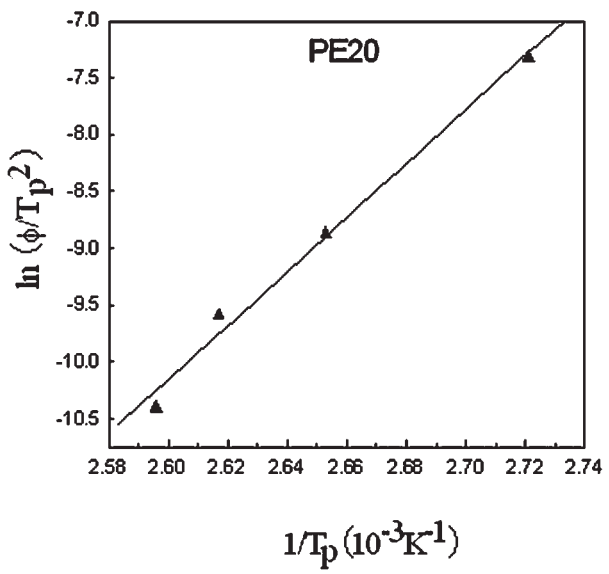

Figure 7 Plots of $\ln(\phi/T_p^2)$ versus $1/T_p$ for PE0 and PE20 samples.

TABLE II
Crystallization Activation Energy of Virgin PE and XLPE Samples

Samples	ΔE_1 (kJ/mol)	R
PE0	176.7	0.987
PE20	197.1	0.995

CONCLUSIONS

1. The Avrami analysis modified by Jeziorny was successful for describing the nonisothermal crystallization process of virgin PE and photocrossinked PE samples.
2. The observation of crystallite structure and kinetics studies revealed that the photocrosslinking impedes the overall nonisothermal crystallization process of PE.

References

1. Qu, B. J.; Shi, W. F.; Liang, R. Y.; Jin, S. Z.; Xu, Y. H.; Wang, Z. H.; Rånby, B. Polym Eng Sci 1995, 35, 1005.
2. Lawton, E. J.; Bueche, A. M.; Balwit, J. S. Nature 1953, 172, 76.
3. Qu, B. J.; Rånby, B. Polym Eng Sci 1995, 35, 1161.
4. Qu, B. J.; Rånby, B. J Appl Polym Sci 1993, 48, 701.
5. Smedber, A.; Hjertberg, T.; Gustafsson, B. Polymer 2003, 44, 3395.
6. Shieh, Y. T.; Tsai, T. H. J Appl Polym Sci 1998, 69, 255.
7. Qu, B. J.; Xu, Y. H.; Shi, W. F.; Rånby, B. Macromolecules 1992, 25, 5215.
8. Qu, B. J.; Xu, Y. H.; Shi, W. F.; Rånby, B. Macromolecules 1992, 25, 5220.
9. Qu, B. J.; Qu, X.; Xu, Y. H.; Jacobsson, U.; Rånby, B.; Russel, K. E.; Baker, W. E. Macromolecules 1997, 30, 1408.
10. Qu, B. J.; Qu, X.; Ding, L. H.; Rånby, B. J Polym Sci Part A: Polym Chem 2000, 38, 999.
11. Qu, B. J.; Rånby, B. J Appl Polym Sci 1993, 48, 711.
12. Qu, B. J.; Rånby, B. J Appl Polym Sci 1993, 49, 1799.
13. Tang, L. X.; Yan, M. Q.; Qu. B. J. J Appl Polym Sci 2006, 99, 2068.
14. Gao, J. G.; Yu, M. S.; Li, Z. T. Eur Polym J 2004, 44, 1533.
15. Hutzler, B. W.; Machado, L. D. B.; Villavicencio, A. L. C. H.; Lugão, A. B. Radiat Phys Chem 2000, 57, 431.
16. Jiao, C. M.; Wang, Z. Z.; Liang, X. M. Polym Test 2005, 24, 75.
17. Gheysari, D.; Behjat, A.; Haji-Saeid, M. Eur Polym J 2001, 37, 296.
18. Avrami, M. J Chem Phys 1940, 8, 212.
19. Jeziorny, A. Polym 1978, 19, 1142.
20. Kissinger, H. E. J Res Natl Stand 1956, 57, 127.